Plates," *Journal of Composite Materials*, Vol. 3, 1969, pp. 148–165.

[9] Ashton, J. E. and Whitney, J. M., *Theory of Laminated Plates*, Technomic, Stamford, Conn., 1970.

[10] Ashton, J. E., "Analysis of Anisotropic Plates—Boundary Conditions," *Journal of Composite Materials*, Vol. 4, 1970, pp. 162–171.

[11] Ashton, J. E., Halpin, J. C., and Petit, P. H., *Primer on Composite Materials: Analysis*, Technomic, Stamford, Conn., 1969.

[12] Doner, D. R. and Novak, R. C., "Structural Behavior of Laminated Graphite Filament Composites," *Proceedings of the SPI*, 24th Annual Technical Conference, Reinforced Plastics/Composites Division, The Society of the Plastics Industry, 1969, Sec. 2-D, p. 1–8.

[13] Lubin, G., ed., *Handbook of Fiberglass and Advanced Plastics Composites*, Van Nostrand-Reinhold, New York, 1970.

[14] Schapery, R. A., "Thermal Expansion Coefficients of Composite Materials Based on Energy Principles," *Journal of Composite Materials*, Vol. 2, 1968, pp. 380–404.

SEPTEMBER 1971 AIAA JOURNAL VOL. 9, NO. 9

Imperfection Sensitivity of Axially Compressed Stringer Reinforced Cylindrical Panels under Internal Pressure

WENDELL B. STEPHENS*
Harvard University, Cambridge, Mass.

This paper is a study of the effects of longitudinal edge stiffness and internal pressure on the buckling and initial postbuckling behavior of axially compressed long cylindrical panels. Two methods of solution are presented. The first is a series solution where the torsional rigidity of the edge stiffeners is not included and the second is a numerical solution where the torsional rigidity of the edge stringers is included. The results show that both internal pressure and the edge stiffener torsional rigidity tend to increase the panel buckling strength and the panel insensitivity to initial imperfections.

Nomenclature

A_n, B_n = coefficients defined in Eq. (35)
a_n, b_n = series coefficients used in Eqs. (29) and (30)
a, b = initial postbuckling coefficient defined in Eq. (8)
c = $\{3(1-\nu^2)\}^{1/2}$
c_0 = arbitrary constant
D = $Et^3/4c^2$
E = Young's modulus
e = constant evolving from Stokes' transformation, see Eq. (31)
$\bar{F}$ = stress function
F = $2c\bar{F}/(Et^3)$, nondimensional stress function
$F^{(0)}, F^{(1)}, F^{(2)}, F_\sigma, F_p$ = defined in Eqs. (3) and (5)
$f(y), f_\alpha(y), f_\beta(y)$ = defined in Eqs. (44) and (19), respectively
K = initial postbuckling parameter defined in Eq. (13)
G = shear modulus of the stiffener
J = torsional constant for the stiffener
$\bar{M}_x, \bar{M}_y, \bar{M}_{xy}$ = bending stress resultants
M_x, M_y, M_{xy} = $(R/2cEt^3)(\bar{M}_x, \bar{M}_y, \bar{M}_{xy})$, nondimensional bending stress resultants
$\bar{N}_x, \bar{N}_y, \bar{N}_{xy}$ = membrane stress resultant
N_x, N_y, N_{xy} = $R/(Et^3)\cdot(\bar{N}_x, \bar{N}_y, \bar{N}_{xy})$, nondimensional membrane stress resultants
$\bar{p}$ = applied internal pressure
p = $\bar{p}R^2c/(Et^2)$
q_0 = $(2cR/t)^{1/2}$
R = cylindrical panel radius
S = series summation defined in Eq. (40)
t = shell thickness
$\bar{U}, \bar{V}, \bar{W}$ = displacements defined in Fig. 1
U, V = $q_0/t(\bar{U}, \bar{V})$, nondimensional displacements
W = $\bar{W}/t$, nondimensional displacement
$W^{(0)}, W^{(1)}, W^{(2)}, W_\sigma, W_p$ = defined in Eqs. (3–5)
w, w_α, w_β = defined in Eqs. (19–43)
$\bar{x}, \bar{y}$ = Cartesian coordinates, see Fig. 1
x = $\bar{x}q_0/R$, nondimensional axial distance
y = $\bar{y}q_0/R$, nondimensional circumferential distance
α = amplitude of $F^{(1)}$, defined by Eq. (15)
β_0 = angle in radians between adjacent stiffeners
γ = $q_0GJ/(DR)$, torsional rigidity parameter
δ = amplitude of buckling displacement, see Eq. (3)
$\bar{\delta}$ = amplitude of a small geometrical imperfection
Δ_0, Δ_n = determinants defined by Eqs. (39) and (35), respectively
θ = $q_0\beta_0/(2\pi)$, flatness parameter
θ_{cr} = value of $\theta(p,\gamma)$ when $b = 0$
Λ = load parameter defined in Eq. (3)
λ = ratio of the wavelength in the y direction to the wavelength in the x direction
ν = Poisson's ratio
$\bar{\sigma}$ = applied axial compressive stress
σ = $\bar{\sigma}Rc/(Et)$, nondimensional axial compressive stress
σ_{cr} = minimum eigenvalue as a function of λ or critical buckling load
σ_s = critical buckling load for an imperfect structure defined in Fig. 2

Received January 18, 1971; revision received May 17, 1971. This work was supported in part by NASA under Grant NGL 22-007-012, and by the Division of Engineering and Applied Physics, Harvard University.

Index Category: Structural Stability Analysis.

* Research Fellow in Structural Mechanics, Division of Engineering and Applied Physics; currently Aerospace Engineer, Automated Methods Section, Design Technology Branch, Structures Division, NASA Langley Research Center, Hampton, Va.

1. Introduction

IN Ref. 1, the buckling and initial postbuckling behavior of an axially compressed narrow cylindrical panel is presented. Such panels occur in longitudinally stiffened

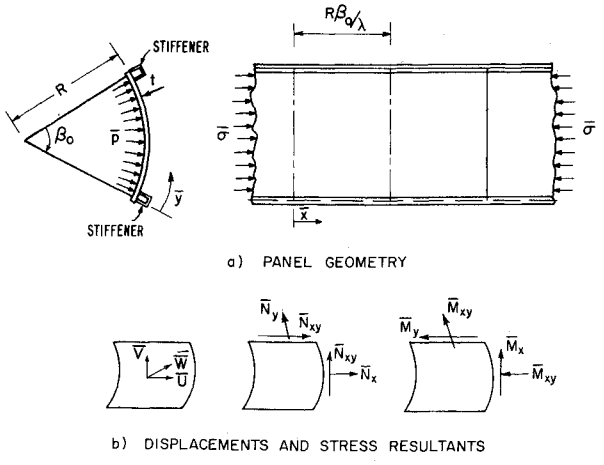

Fig. 1 Panel geometry and sign convention.

cylinders. In that study it was found that the panels, whose geometry was described by a "flatness" parameter θ, have stable initial postbuckling behavior for values of θ less than 0.64. Here, θ is defined as

$$\theta = q_0\beta_0/2 \tag{1}$$

where β_0 is the panel central angle in radians between adjacent equally spaced stringers and q_0 is a measure of the shell radius to thickness ratio. The analysis was limited to values of θ less than 1. This is because the problem is characterized by a unique buckling mode only for values of θ less than 1. For those values, the panel buckling stress is higher than that of the unstiffened cylinders. For wide panels ($\theta \geq 1.0$), there is no unique buckling mode and the buckling stress is equal to that of the unstiffened cylinder.

This study extends the work in Ref. 1 to include the torsional rigidity of the stringers and internal pressure on the panel. It was expected in Ref. 1 that the inclusion of torsional rigidity of the stringers would have two effects: 1) it would increase the upper limit on θ in which unique modes would occur, and 2) it would also increase the limiting value of θ for which there is stable postbuckling behavior. Both of these effects are studied in this paper.

The problem is studied within the context of the Kármán-Donnell equations, described by two dependent variables; W, the normal deflection, and F, the stress function. The analysis is based on Koiter's general theory of postbuckling behavior, which is presented concisely in Refs. 2 and 3.

Two separate methods for solving the governing equations are presented. First, the problem with internal pressure but without torsional rigidity is solved by means of a serious solution. This method of solution was applied to Koiter's original narrow panel problem by Budiansky[4] and is extended here to include internal pressure. The second method is a numerical solution to the problem which includes both the torsional rigidity of the stringers and an internal pressure on the panel. For this case, a series solution is not tractable and a numerical method is required.

2. Buckling and Initial Postbuckling Analysis

The nondimensional Kármán-Donnell equations for a cylindrical panel subjected to a nondimensional internal pressure p are

$$\begin{aligned} \nabla^4 W + F'' &= 2c\{F''W'' + F''W'' - 2F'W'\} + p/c \\ \nabla^4 F - W'' &= 2c\{W''W'' - W'^2\} \end{aligned} \tag{2}$$

where W is the nondimensional deflection and F is the nondimensional Airy stress function. Here F is related to the nondimensional stress resultants by $F'' = N_x, F'' = N_y, F' = -N_{xy}$. The primes and dots represent, respectively, derivatives with respect to the nondimensional axial distance x and the nondimensional circumferential distance y. The symbol $\nabla^4(\ )$ is defined in the usual manner as $\{(\ )'' + (\ )''\}^2$. The constant c and the relationship between dimensional and nondimensional variables are defined in the nomenclature. The sign convention is described in Fig. 1. The reworked version of Koiter's general theory of buckling and postbuckling analysis previously described[2] assumes asymptotic expansions for W,F of the form

$$\begin{Bmatrix} W \\ F \end{Bmatrix} = \Lambda \begin{Bmatrix} W^{(0)} \\ F^{(0)} \end{Bmatrix} + \frac{\delta}{t} \begin{Bmatrix} W^{(1)} \\ F^{(1)} \end{Bmatrix} + \left(\frac{\delta}{t}\right)^2 \begin{Bmatrix} W^{(2)} \\ F^{(2)} \end{Bmatrix} + \cdots \tag{3}$$

where $W^{(0)},F^{(0)}$ defines the prebuckled state and $W^{(1)},F^{(1)}$ describe the buckling mode. The quantities $W^{(2)},F^{(2)}$ and higher order terms are orthogonal to the buckling mode. The scalar Λ is a loading parameter with which the loading increases proportionally. In the present problem, however, the internal pressure is held fixed, while only the axial stress is allowed to vary proportionally. Thus, Eq. (3) for the present problem becomes

$$\begin{Bmatrix} W \\ F \end{Bmatrix} = \begin{Bmatrix} W_p \\ F_p \end{Bmatrix} + \sigma \begin{Bmatrix} W_\sigma \\ F_\sigma \end{Bmatrix} + \frac{\delta}{t} \begin{Bmatrix} W^{(1)} \\ F^{(1)} \end{Bmatrix} + \left(\frac{\delta}{t}\right)^2 \begin{Bmatrix} W^{(2)} \\ F^{(2)} \end{Bmatrix} + \cdots \tag{4}$$

Here the prebuckling state is represented by a membrane stress state and the deflection is approximated to sufficient accuracy by a constant such that

$$W_p = p/c \qquad F_p = \tfrac{1}{2}p/cx^2 \tag{5a}$$

and

$$W_\sigma = \nu/c \qquad F_\sigma = -\tfrac{1}{2}y^2/c \tag{5b}$$

where σ is the average nondimensional axial compressive stress and is regarded as the load parameter. The first-order set of equations describes the classical eigenvalue problem for the critical load parameter σ_{cr}, and is given by

$$\nabla^4 W^{(1)} + F^{(1)''} - 2pW^{(1)\cdot\cdot} + 2\sigma_{cr}W^{(1)''} = 0 \tag{6}$$

$$\nabla^4 F^{(1)} - W^{(1)''} = 0 \tag{7}$$

where $W^{(1)}$ is chosen such that its maximum value is unity.

In the postbuckling region, it is shown in Refs. 2 and 3 that

$$\sigma/\sigma_{cr} = 1 + a\delta/t + b(\delta/t)^2 + \cdots \tag{8}$$

This relation is necessarily symmetric for the present problem since there are many waves in the x direction. Therefore, $a = 0$. A general expression for b, the postbuckling parameter, is given in Ref. 2; for this problem, it reduces to

$$\begin{aligned} b = c\iint [2\{&F^{(1)\cdot\cdot}W^{(1)'}W^{(2)'} + F^{(1)''}W^{(1)\cdot}W^{(2)\cdot} - \\ &F^{(1)\cdot'}(W^{(1)'}W^{(2)\cdot} + W^{(1)\cdot}W^{(2)'})\} + \{F^{(2)\cdot\cdot}(W^{(1)'})^2 + \\ &F^{(2)''}(W^{(1)\cdot})^2 - 2F^{(2)\cdot'}W^{(1)'}W^{(1)\cdot}\}]dx\,dy \div \\ &\iint \sigma_{cr}(W^{(1)'})^2 dx\,dy \end{aligned} \tag{9}$$

Here the second-order terms $W^{(2)},F^{(2)}$ are required for the evaluation of b. Using Eqs. (2,4,6–8), and $a = 0$, the governing equations for $W^{(2)}$ and $F^{(2)}$ are

$$\begin{aligned} \nabla^4 W^{(2)} + F^{(2)''} - 2pW^{(2)\cdot\cdot} + 2\sigma_{cr}W^{(2)''} = \\ 2c\{F^{(1)\cdot\cdot}W^{(1)''} + F^{(1)''}W^{(1)\cdot\cdot} - 2F^{(1)\cdot'}W^{(1)\cdot'}\} \end{aligned} \tag{10}$$

$$\nabla^4 F^{(2)} - W^{(2)''} = -2c\{W^{(1)''}W^{(1)\cdot\cdot} - W^{(1)\cdot'^2}\} \tag{11}$$

If b is positive, the initial postbuckling behavior will not be very sensitive to small imperfections and the initial postbuckling behavior is stable. If b is negative, the structure

is sensitive to small geometrical imperfections that can greatly reduce the buckling load. Koiter obtained an expression for the static buckling strength σ_s of a structure with an initial midsurface imperfection of magnitude $\bar{\delta}$ and with a shape corresponding to the classical buckling mode. Suppose the structure, when perfect, obeys the symmetric load-postbuckling deflection relation ($a = 0$) given by Eq. (8); Koiter's result for the imperfect structure, which is asymptotically valid for small $\bar{\delta}$, is

$$(1 - \sigma_s/\sigma_{cr})^{3/2} = [3(3)^{1/2}/2](-b)^{1/2}[\sigma_s/\sigma_{cr}|\bar{\delta}/t| \quad (12)$$

The symmetric postbuckling behavior of the structure with a small initial geometric imperfection and b negative is depicted by the dotted line in Fig. 2. Thus, the loss in buckling strength is of the order of $(\bar{\delta}/t)^{2/3}$. Another parameter used in Refs. 1 and 2 to demonstrate the initial postbuckling behavior is the initial postbuckling stiffness parameter K. This parameter is defined conveniently in Ref. 2 and, for this problem, becomes

$$K = \left\{1 + \frac{c^2 \iint W^{(1)\prime 2} dxdy}{b\sigma_{cr} \iint dxdy}\right\}^{-1} \quad (13)$$

The parameter K is the ratio of the postbuckling stiffness to the prebuckling stiffness and gives the initial postbuckling slope of the load-end shortening curve.

3. Panel Buckling with Torsional Rigidity of Stiffeners Neglected: Series Solution

The solution for the panel buckling and postbuckling behavior without torsional rigidity requires certain simplifying assumptions along the shell boundaries. Since the panel is very long, the boundary conditions at the panel ends have no appreciable effect and solutions that are periodic in the axial direction x are sought. At the boundaries $y = 0$, $q_0\beta_0$, the edges are assumed to remain straight and both the flexural rigidity in the tangential direction and the torsional rigidity of the stiffeners are neglected. These conditions coupled with the evenness of the tangential displacement V about the stiffener, yield the following boundary conditions on $W^{(1)}$ and $F^{(1)}$:

$$\left.\begin{aligned} F^{(1)} &= F^{(1)\cdot\cdot} = 0 \\ W^{(1)} &= W^{(1)\cdot\cdot} = 0 \end{aligned}\right\}, \; y = 0, \; q_0\beta_0 \quad (14)$$

These conditions are satisfied by assuming solutions to Eqs. (6) and (7) of the form

$$\begin{aligned} W^{(1)} &= \sin\lambda x/2\theta \sin y/2\theta \\ F^{(1)} &= \alpha \sin\lambda x/2\theta \sin y/2\theta \end{aligned} \quad (15)$$

where $\theta = q_0\beta_0/2\pi$. Here α is the amplitude of $F^{(1)}$ and the amplitude of $W^{(1)}$ is set to unity. Since it is anticipated that there be only one half-wave in the y direction, then λ can be interpreted to be the ratio of the buckling wave length in the y direction to the buckling wavelength in the x direction. By substituting Eqs. (15) into Eqs. (6) and (7), the values of α and the eigenvalue σ_{cr} become

$$\alpha = -4\theta^2/\Omega \quad (16)$$

$$\sigma_{cr} = (1/8\theta^2)\{\Omega + 16\theta^4/\Omega\} + p/\lambda^2 \quad (17)$$

where

$$\Omega = (\lambda^2 + 1)^2/\lambda^2$$

To obtain the minimum eigenvalue, Eq. (17) is minimized with respect to λ. The result yields the value of λ, which, for a given pressure p, minimizes σ_{cr}. It is algebraically much simpler, however, to use the resulting expression as a definition of pressure for a given λ. This result is

$$p = (1/8\theta^2)\{1 - 16\theta^4/\Omega^2\}\{\lambda^4 - 1\} \quad (18)$$

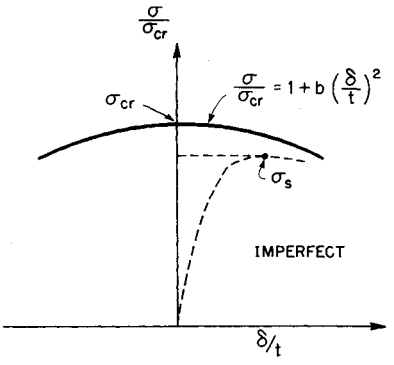

Fig. 2 Buckling of imperfection sensitive shells.

Equations (10) and (11), which govern second-order nonhomogeneous boundary-value problems, contain quadratic terms of $W^{(1)}$ and $F^{(1)}$, which are either independent of the x coordinate or proportional to $\cos(\lambda x/\theta)$. This implies that the solution to Eqs. (10) and (11) can be written in the separated form of

$$W^{(2)} = c\{w_\alpha(y) + w_\beta(y) \cos\lambda x/\theta\} \quad (19a)$$

$$F^{(2)} = c\{f_\alpha(y) + f_\beta(y) \cos\lambda x/\theta\} \quad (19b)$$

By substituting Eqs. (19) into Eqs. (10) and (11), the following two sets of ordinary differential equations are derived:

$$w_\alpha^{\cdot\cdot\cdot\cdot} - 2pw_\alpha^{\cdot\cdot} = \tfrac{1}{2}(\lambda^2/\Omega)(1/\theta^2) \cos y/\theta \quad (20)$$

$$f_\alpha^{\cdot\cdot\cdot\cdot} = (\lambda^2/16\theta^4) \cos(y/\theta) \quad (21)$$

and

$$w_\alpha^{\cdot\cdot\cdot\cdot} - 2\left\{\left(\frac{\lambda}{\theta}\right)^2 + p\right\} w_\beta^{\cdot\cdot} + \left\{\left(\frac{\lambda}{\theta}\right)^4 - 2\sigma_c\left(\frac{\lambda}{\theta}\right)^2\right\} w_\beta - \left(\frac{\lambda}{\theta}\right)^2 f_\beta = \frac{1}{2\Omega}\left(\frac{\lambda}{\theta}\right)^2 \quad (22)$$

$$f_\beta^{\cdot\cdot\cdot\cdot} - 2\left(\frac{\lambda}{\theta}\right)^2 f_\beta^{\cdot\cdot} + \left(\frac{\lambda}{\theta}\right)^4 f_\beta + \left(\frac{\lambda}{\theta}\right)^2 w_\beta = \frac{\lambda^2}{16\theta^4} \quad (23)$$

The boundary conditions for Eqs. (20) and (21) are

$$\begin{aligned} w_\alpha^{\cdot} = f_\alpha^{\cdot\cdot\cdot} &= 0, \; y = 0 \\ w_\alpha^{\cdot} = w_\alpha^{\cdot\cdot\cdot} = f_\alpha^{\cdot} = f_\alpha^{\cdot\cdot\cdot} &= 0, \; y = q_0\beta_0/2 \end{aligned} \quad (24)$$

and for Eqs. (22) and (23),

$$\begin{aligned} w_\beta = w_\beta^{\cdot} = f_\beta^{\cdot} = f_\beta^{\cdot\cdot\cdot} &= 0, \; y = 0 \\ w_\beta^{\cdot} = w_\beta^{\cdot\cdot\cdot} = f_\beta^{\cdot} = f_\beta^{\cdot\cdot\cdot} &= 0, \; y = q_0\beta_0/2 \end{aligned} \quad (25)$$

Since the circumferential displacement must be single-valued for any complete circumferential circuit, an additional boundary condition is derived from

$$\oint V_{,y}\, dy = 0 \quad (26)$$

which implies that

$$\int_0^{q_0\beta_0} w_\alpha dy = \frac{-q_0\beta_0}{16\theta^2} \quad (27)$$

This additional condition with Eqs. (24) uniquely defines w_α and f_α and is determined to within an arbitrary constant. Thus, the solutions to Eqs. (20) and (21) with boundary conditions (24) and (27) are

$$\begin{aligned} w_\alpha &= -1/16\theta^2 + [\theta^2\lambda^2/2\Omega(1 + 2\theta^2 p)] \cos y/\theta \\ f_\alpha &= c_0 + (\lambda^2/16) \cos y/\theta \end{aligned} \quad (28)$$

where c_0 is an arbitrary constant. The constant c_0 need not be determined since an inspection of Eq. (9) shows that only second derivatives of f_α are required for the postbuckling analysis.

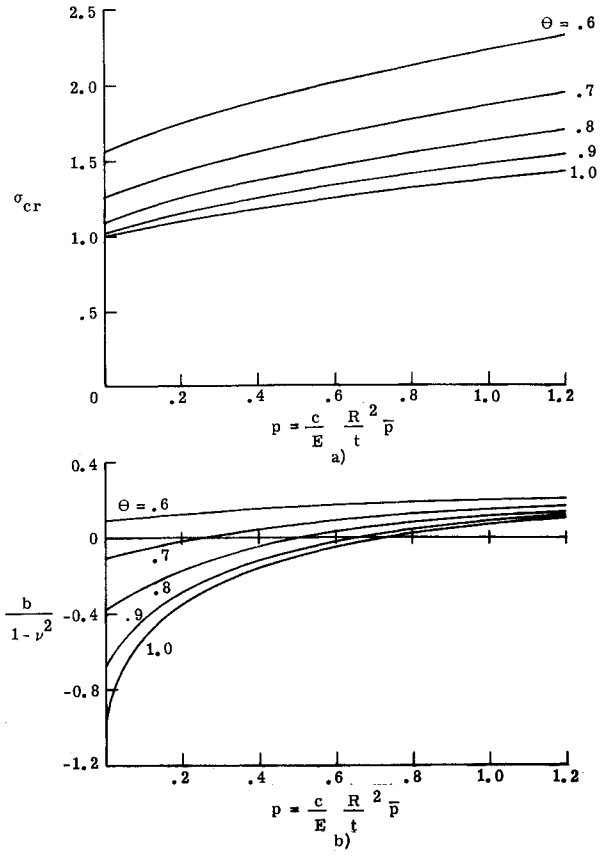

Fig. 3 Critical stress σ_{cr} and initial imperfection sensitivity b vs internal pressure p for various values of θ at $\gamma = 0$.

Solutions to Eqs. (22) and (23) with boundary conditions (24) are assumed to be the infinite series

$$w_\beta = \sum_{n=0,1}^{\infty} a_n \cos\frac{n}{\theta} y \tag{29}$$

$$f_\beta = \sum_{n=0,1}^{\infty} b_n \cos\frac{n}{\theta} y \tag{30}$$

Each term of f_β satisfies the boundary conditions so differentiation can be interchanged with summation. Each term of w_β, however, does not satisfy the boundary conditions, and it is necessary to use Stokes transformations to express the fourth derivative of w_β as

$$w_\beta'''' = \frac{e}{2} + \sum_{n=1,2}^{\infty} \left[e + \left(\frac{n}{\theta}\right)^4 a_n\right] \cos\frac{n}{\theta} y \tag{31}$$

where e is a constant to be determined. Equations (29–31) are substituted into Eqs. (22) and (23), yielding two equations for a_0 and b_0 in terms of the constant e and $2n$ equations for a_n and b_n when $n > 0$. The condition that the stiffener edges remain straight yields the extra condition for determining e. This condition becomes

$$a_0 = -\sum_{n=1,2}^{\infty} a_n \tag{32}$$

The coefficients a_n and b_n from the $2n$ equations become

$$a_n = -e(\theta/\lambda)^2 B_n/\Delta_n \tag{33}$$

$$b_n = e(\theta/\lambda)^2 1/\Delta_n \tag{34}$$

where

$$\Delta_n = A_n B_n + 1, \quad A_n = B_n + 2p(n/\lambda)^2 - 2\sigma_{cr}$$
$$B_n = (\theta/\lambda)^2\{(n/\theta)^2 + (\lambda/\theta)^2\}^2 \tag{35}$$

when $n > 0$. Also from the two equations when $n = 0$ and Eq. (32), the definitions a_0,b_0, and e are obtained as follows:

$$a_0 = (S/2\Delta_0\theta^2)\{1/8\theta^2 + (\lambda/\theta)^2 1/\Omega\} \tag{36}$$

$$b_0 = \frac{1}{2\Delta_0\theta^2}\left(S\left[\frac{1}{\Omega} - \frac{1}{8\theta^2}\left\{\left(\frac{\lambda}{\theta}\right)^2 - 2\sigma_{cr}\right\}\right] - \frac{1}{16}\right) \tag{37}$$

$$e = (-1/2\Delta_0)(\lambda/\theta)^2\{1/8\theta^2 + 1/\Omega(\lambda/\theta)^2\} \tag{38}$$

where

$$\Delta_0 = -\left\{\left(\frac{\lambda}{\theta}\right)^4 - 2\left(\frac{\lambda}{\theta}\right)^2 \sigma_{cr} + 1\right\}\frac{S}{\theta^2} - \frac{1}{2}\left(\frac{\lambda}{\theta}\right)^2 \tag{39}$$

and for brevity

$$S = \theta^2 \sum_{n=1,2}^{\infty} \frac{B_n}{\Delta_n} \tag{40}$$

Thus the second-order solution is now complete in terms of the summation S.

The expression for the postbuckling parameter b in Eq. (9) is now integrated using Eqs. (15,28–30) to yield

$$\frac{b}{(1-\nu^2)} = \frac{3}{2\theta^2\sigma_{cr}}\left\{\frac{\lambda^2}{16} + b_0 - \frac{8\theta^2}{\Omega} \times \left(a_0 + \frac{\theta^2\lambda^2}{2\Omega(1+2\theta^2 p)}\right)\right\} \tag{41}$$

And finally the postbuckling stiffness parameter K becomes

$$K = \{1 + c^2\lambda^2/16\theta^2 b\sigma_{cr}\}^{-1} \tag{42}$$

For the case where $p = 0$ and $\lambda = 1$, Eqs. (40–42) reduce to those results given in Refs. 1 and 4.

4. Panel Buckling with Torsional Rigidity: Numerical Solution

The problem is now solved with the torsional rigidity of the longitudinal edge stiffeners included. This inclusion changes the buckle shape from the simple sinusoidal deflection in the y direction, and the series solution for this problem is extremely laborious. Therefore, a numerical solution in the y direction is used. Thus, separated solutions to Eqs. (6) and (7) of the form

$$W^{(1)} = w(y)\cos(\lambda/2\theta)x \tag{43}$$

$$F^{(1)} = f(y)\cos(\lambda/2\theta)x \tag{44}$$

are sought where the variables w and f are solved for numerically.

This method was used on a similar problem by Hutchinson.[5] Equations (6) and (7) with Eqs. (43) and (44) give

$$w'''' - 2\left\{\left(\frac{\lambda}{2\theta}\right)^2 + p\right\} w'' + \left\{\left(\frac{\lambda}{2\theta}\right)^4 - 2\left(\frac{\lambda}{2\theta}\right)^2 \sigma_{cr}\right\} w - \left(\frac{\lambda}{2\theta}\right)^2 f = 0 \tag{45}$$

$$f'''' - 2\left(\frac{\lambda}{2\theta}\right)^2 f'' + \left(\frac{\lambda}{2\theta}\right)^4 f + \left(\frac{\lambda}{2\theta}\right)^2 w = 0 \tag{46}$$

which are ordinary homogeneous equations in f and w. The boundary conditions at $y = 0$ are similar to those in Eqs. (14) except for the second condition on $W^{(1)}$. Here the panel edge bending moment is set equal to the torsional moment in

the stringer. This condition reduces to

$$[(GJ/DR)q_0]W^{(1)\prime\cdot} = -2W^{(1)\cdot\cdot} \quad (47)$$

where G is the stiffener shear modulus, J is the stiffener torsion constant, R is the cylindrical panel radius and D is the panel bending stiffness defined by $D = Et^3/4c^2$. Here, a free torsion (unconstrained) model of the stiffener was used. There is no twisting of the stiffener in the prebuckled state since deformation of the cylinder is axisymmetric. The boundary condition (47) is for the buckling state and assumes that the stiffener is free to twist throughout its length. In terms of w and f, the boundary conditions at $y = 0$ are

$$f = f^{\cdot\cdot} = 0,\ w = 0,\ (\lambda^2/8\theta^2)\gamma w^{\cdot} - w^{\cdot\cdot} = 0 \quad (48)$$

where $\gamma = q_0GJ/(DR)$. As before, it is convenient to make use of the symmetry of the eigenmode at $y = q_0\beta_0/2$. These conditions become

$$w^{\cdot} = w^{\cdot\cdot\cdot} = 0 \qquad f^{\cdot} = f^{\cdot\cdot\cdot} = 0 \quad (49)$$

Equations (45) and (46) and the boundary conditions (48) and (49) are represented numerically using central differences, and the determinant is found by using a Potter's method of Gaussian elimination. The critical σ for a given value of λ occurs when the determinant is zero. The classical buckling stress σ_{cr} is the minimum value of the critical σ which occurs over all λ. The amplitude of w at $y = q_0\beta_0/2$ is taken to be unity and the functions of w and f are determined.

The solutions of the second-order equations (10) and (11) again written in the separated form of Eqs. (19). These equations are reduced to the following sets of ordinary nonhomogeneous equations:

$$w_\alpha^{\cdot\cdot\cdot\cdot} - 2pw_\alpha^{\cdot\cdot} = -(\lambda/2\theta)^2(fw)^{\cdot\cdot} \quad (50)$$

$$f_\alpha^{\cdot\cdot\cdot\cdot} = (\lambda/2\theta)^2[w^{\cdot\cdot}w - w^{\cdot 2}] \quad (51)$$

and

$$w_\beta^{\cdot\cdot\cdot\cdot} - \left\{8\left(\frac{\lambda}{2\theta}\right)^2 + 2p\right\} w_\beta^{\cdot\cdot} + \left\{16\left(\frac{\lambda}{2\theta}\right)^4 - 8\left(\frac{\lambda}{2\theta}\right)^2 \sigma_{cr}\right\} w_\beta - 4\left(\frac{\lambda}{2\theta}\right)^2 f_\beta = -\left(\frac{\lambda}{2\theta}\right)^2 \{fw^{\cdot\cdot} + f^{\cdot\cdot}w - 2f^{\cdot}w^{\cdot}\} \quad (52)$$

$$f_\beta^{\cdot\cdot\cdot\cdot} - 8\left(\frac{\lambda}{2\theta}\right)^2 f_\beta^{\cdot\cdot} + 16\left(\frac{\lambda}{2\theta}\right)^4 f_\beta + 4 \times \left(\frac{\lambda}{2\theta}\right)^2 w_\beta = \left(\frac{\lambda}{2\theta}\right)^2 \{ww^{\cdot\cdot} - w^{\cdot 2}\} \quad (53)$$

The equation for the postbuckling parameter b reduces to

$$\frac{b}{(1-\nu^2)} = 6\int_0^{q_0\beta_0/2} \left\{-fw^{\cdot}\left(w_\alpha^{\cdot} + \frac{1}{2}w_\beta^{\cdot}\right) + f^{\cdot\cdot}ww_\beta - f^{\cdot}w\left(w_\alpha^{\cdot} - \frac{1}{2}w_\beta^{\cdot}\right) - f^{\cdot}w^{\cdot}w_\beta - f_\beta w^{\cdot 2} + \frac{1}{2}\left(f_\alpha^{\cdot\cdot} - \frac{1}{2}f_\beta^{\cdot\cdot}\right)w^2 - f_\beta^{\cdot}ww^{\cdot}\right\} dy \div \int_0^{q_0\beta_0/2} \sigma_{cr}w^2 dy \quad (54)$$

where only first derivatives of w_α and the second derivatives of f_α are required. The boundary conditions on Eqs. (50) and (51) are identical to those given in Eq. (24). It is important to observe that the second-order deflection $W^{(2)}$ does not tend to twist the stiffener but instead is an even function about the stiffener.

Thus Eqs. (50) and (51) with the boundary conditions (24) are uncoupled ordinary nonhomogeneous differential equations that are solved numerically for $\dot{w}_\alpha$ and $\dot{f}_\alpha$ using the quadratic terms of w and f given from the first-order solutions.

The boundary conditions on Eqs. (52) and (53) are identical to those given in Eqs. (25). These equations are also solved numerically using the Potter's Gaussian elimination scheme.

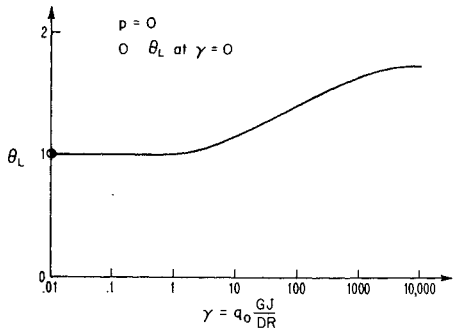

Fig. 4 Limiting values of θ for which the analysis is valid as a function of $\gamma(p = 0)$.

5. Results and Discussion

In Fig. 3 the results for σ_{cr} and b are plotted as a function of internal pressure p for several values of θ. The results agree with those presented by Koiter[1] for σ_{cr}, b, and K when internal pressure is zero. The curves show that increasing the internal pressure tends to increase σ_{cr} and also to make the panel more insensitive to initial imperfections. The value θ at which $b = 0$ is defined as θ_{cr}. The amount of pressure required to obtain θ_{cr} increases with increasing θ. These results correspond to the series solution being summed over the first 40 terms.

In Figs. 4–8, the effect of the edge stiffener torsional rigidity on buckling and initial postbuckling behavior is included in the analysis as well as the internal pressure on the panel. These results were obtained using the numerical approach with 30 finite difference increments taken from $y = 0$

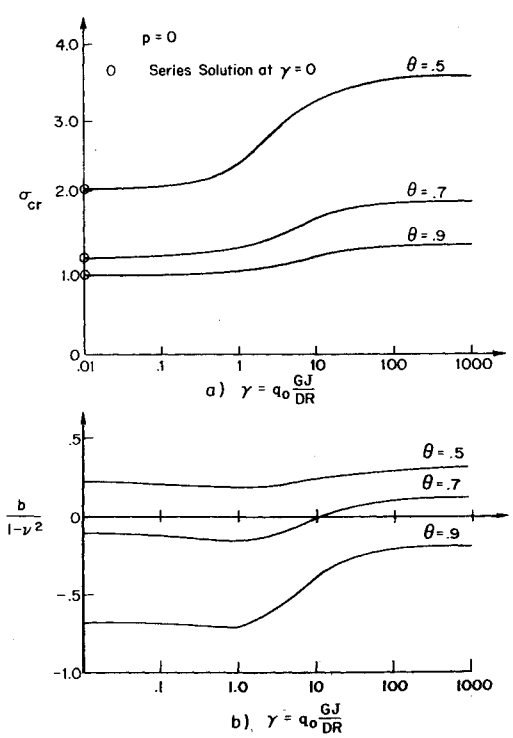

Fig. 5 Critical stress σ_{cr} and initial imperfection sensitivity b vs γ for various values of θ and $p = 0$.

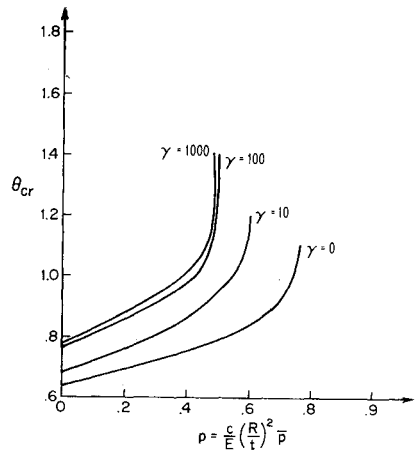

Fig. 6 Plot of θ_{cr} as a function of internal pressure p for various values of torsional rigidity γ.

to $y = q_0\beta_0/2$. The numerical results and the series solutions agreed to within 1% for the cases where $\gamma = 0$.

Figure 4 shows the limiting values of θ denoted as θ_L for which the analysis is valid. It was shown in Ref. 1 that θ could not exceed 1, since for higher values of θ, the analysis would produce nonunique solutions. It was suggested in Ref. 1, however, that the torsional stiffness parameter γ would increase the range over which the analysis is valid. The validity of this suggestion is demonstrated by the curve in Fig. 4. Points lying in the region below the solid curve are those included in this analysis. The emergence of more than one minimum for σ as a function of λ was clearly noted when θ exceeded θ_L when the pressure was zero. This phenomenon did not appear when values of pressure greater than zero were introduced and, therefore, the curve was obtained only for the value of $p = 0$.

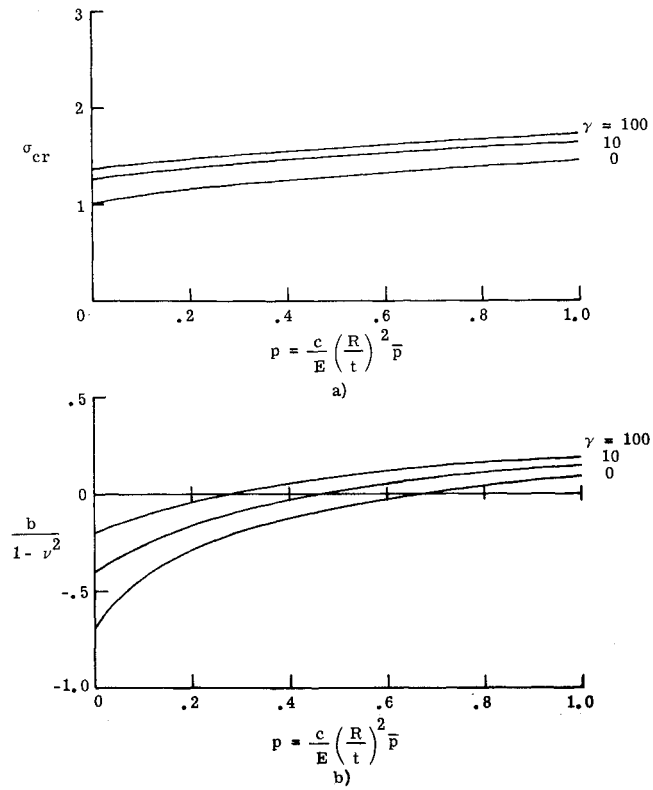

Fig. 7 Typical curves for θ_{cr} and b at $\theta = 0.9$ as a function of internal pressure and for various values of torsional rigidity γ.

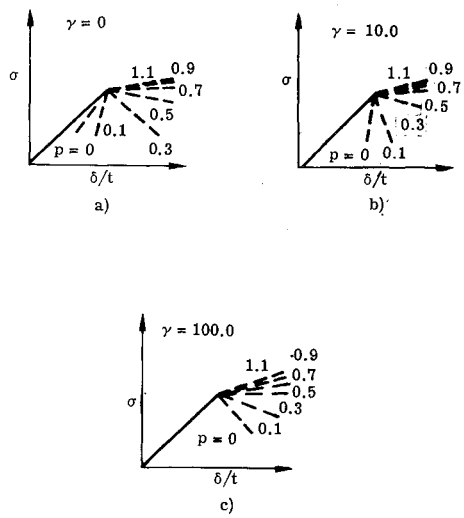

Fig. 8 Typical initial postbuckling slopes $\theta = 0.9$ for values of torsional rigidity γ and internal pressure.

Figure 5 shows the buckling stress and postbuckling behavior obtained when plotted as a function γ for various values of θ. These curves are again computed when the pressure is zero. The open circles along the ordinate of the graphs represent solutions to the case when $\gamma = 0$ which is equivalent to a panel with pinned edges. A large value of γ approaches the case where the panel is clamped along the edge. The inclusion of the γ term increases the critical stress and moves the sensitivity parameter b toward a more positive value. A large value of γ, however, will not necessarily make b positive as is shown for the $\theta = 0.9$ case; but its magnitude is reduced considerably. As discussed by Koiter,[1] wing panels have values of θ considerably smaller than $\theta = 0.5$, and fuselage panels are normally in the range of $0.4 \leq \theta \leq 2.0$. Thus, the large effects of γ on the σ_{cr} for low values of θ and on the b parameter for larger values of θ are, indeed, advantageous, since in practical applications it is expected that γ will vary from 10 to 100. The increase in σ_{cr} as a function of γ at $\theta = 0.5$ is about 65%, and larger increases may be expected for smaller values of θ. On the other hand, at $\theta = 0.9$, the largest value of θ presented, the increase in σ_{cr} is small, while the change in b is greatest and is tending toward less instability in the initial postbuckling behavior.

Figure 6 is a cross plot of many of the features noted in Figs. 3 and 5. Here, for various values of γ, the θ_{cr}, which is the value of θ at zero imperfection sensitivity, are plotted as a function of internal pressure. The regions above the solid curves are the regions of imperfection sensitivity. As was suggested by Fig. 5, the regions of sensitivity in Fig. 6 decrease with increasing γ up to a point of about $\gamma = 1000$. Higher values of γ are expected to reduce the sensitivity region very little. It is interesting to observe that initially even a small value of γ (say $\gamma = 10$) decreases the sensitivity region significantly from the $\gamma = 0$ curve.

Figure 7 shows graphically the effect of γ and pressure on σ_{cr} and b for the particular value of $\theta = 0.9$. As was indicated previously, σ_{cr} increases with increasing both γ and pressure. Actually, the increase in σ_{cr} as a function of pressure is almost linear for each value of γ. Also at $\gamma = 100$, the pressure required to yield a value of $b = 0$ is about 60% lower than at $\gamma = 0$. Even the low value of $\gamma = 10$ reduces this pressure over 30%.

Finally, in Fig. 8 the $\theta = 0.9$ case is again presented showing the effects of pressure on the initial postbuckling slope K for various values of γ. This parameter indicates the initial direction of displacement after buckling has occurred. The prebuckled slope is the solid line and the initial post-

buckling slopes are given by the dashed lines. The combined effects of increasing γ and pressure increase the direction of initial postbuckling from an extreme slope almost doubling back on the original prebuckling displacement curve to a slope of roughly half that of the prebuckled slope. The wide variation in initial postbuckling slopes shown in Fig. 8a can be expected to decrease as θ decreases. The extreme slopes at low pressure move counterclockwise with decreasing θ, while the limiting slope at high pressure changes very slightly. For example, the $\theta = 0.7$ case for $\gamma = 0$ closely approximates that given in Fig. 8c.

6. Concluding Remarks

The effects of internal pressure and edge stiffener torsional rigidity on buckling and initial postbuckling behavior have been presented. The study is conducted within the context of the Kármán-Donnell equations and Koiter's initial postbuckling theory. It has been shown that even moderate values of torsional rigidity significantly reduce the panel imperfection sensitivity. An internal pressure can also aid in making the panel more insensitive to small geometric imperfections. In addition, the values of the panel flatness parameter for which the analysis is valid is increased by including the torsional rigidity of the stiffener. In the limit where torsional rigidity and internal pressure are zero, the present results reduce exactly to the original results of Koiter.

References

[1] Koiter, W. T., "Buckling and Postbuckling Behavior of a Cylindrical Panel Under Axial Compression," Rept. S.476, 1956, National Aeronautical Research Institute, Amsterdam.

[2] Budiansky, B., "Post-Buckling Behavior of Cylinders in Torsion," *IUTAM Symposium, Copenhagen, 1967, Theory of Thin Shells*, edited by F. I. Niordson, Springer-Verlag, New York, 1969.

[3] Budiansky, B. and Amazigo, J. C., "Initial Postbuckling Behavior of Cylindrical Shells Under External Pressure," *Journal of Mathematics and Physics*, Vol. 47, No. 3, Sept. 1968, pp. 223–235.

[4] Budiansky, B., unpublished lecture notes, 1969, Harvard Univ., Cambridge, Mass.

[5] Hutchinson, J. W., "Buckling and Initial Postbuckling Behavior of Oval Cylindrical Shells Under Axial Compression," *Transactions of the ASME: Ser. E*, Vol. 35, No. 1, March 1968, pp. 66–72.

SEPTEMBER 1971 AIAA JOURNAL VOL. 9, NO. 9

Finite-Element Analysis of Large Elastic-Plastic Transient Deformations of Simple Structures

RICHARD W. H. WU* AND EMMETT A. WITMER†
Massachusetts Institute of Technology, Cambridge, Mass.

The assumed-displacement finite-element method which is based upon the Principle of Virtual Work is extended to analyze the large-deflection transient responses of simple structures including elastic-plastic, strain-hardening, and strain-rate material behavior. The resulting equations of motion are solved by a direct timewise numerical integration scheme using the central-difference procedure. Numerical examples are carried out and compared with both finite-difference predictions and experimental results for an impulsively loaded beam and an impulsively loaded ring.

Introduction

THE conventional closed form analysis/prediction of structural transient responses which involve large deformations and nonlinear material behavior is rendered practically impossible by the complexities arising from these two sources of nonlinearities. In practice, therefore, one is usually forced to employ numerical prediction methods.

Numerical methods of structural analysis may be described conveniently in two categories. In the first category is the "finite-element method" which is most systematically based upon variational principles[1]; the solid continuum is idealized as an assemblage of a finite number of regions which are connected at a finite number of nodes along interelement (or interregion) boundaries, with the geometry and the material properties of the continuum being faithfully retained in the idealized structural assembly. The second category, "the numerical solution of the governing algebraic and/or differential equations," is based upon mathematically approximating and solving the differential equations by either finite differences[2–4] or by numerical integration.[5–7] In the past several years, the finite-element method has undergone intensive development and has proved to be a very effective and powerful method for analyzing certain classes of problems such as small-deflection, linear-elastic, static, and dynamic response behavior.[8–11] For predicting large-deflection, elastic-plastic transient response of structures, the finite-difference approach[3,4,12–14] has been much more extensively developed than the finite-element method; corresponding developments of the finite-element method to treat this class of problems would be valuable. A contribution to this area is the subject of this study.

Among the finite-element analyses for large-deflection linear-elastic behavior including both static and transient responses are the developments reported in Ref. 15 for shells of revolution. In Ref. 15, large deflection terms are treated as equivalent force terms which are derived from the pertinent energy expressions in the variational formulation employed; for those special terms, a linear rather than a cubic displacement field for the normal displacement is used in order to

Received September 21, 1970, revision received January 4, 1971.

* Graduate Student in the Aeroelastic and Structures Research Laboratory (MIT-ASRL) of the Department of Aeronautics and Astronautics.

† Professor of Aeronautics and Astronautics.